ACR No. 4B22

NATIONAL ADVISORY COMMITTEE FOR AERONAUTICS

WARTIME REPORT

ORIGINALLY ISSUED
February 1944 as
Advance Confidential Report 4B22

THE DETERMINATION OF SPAN LOAD DISTRIBUTION AT HIGH SPEEDS BY USE OF HIGH-SPEED WIND-TUNNEL SECTION DATA

By John Boshar

Langley Memorial Aeronautical Laboratory
Langley Field, Va.

NACA

WASHINGTON

NATIONAL ADVISORY COMMITTEE FOR AERONAUTICS

ADVANCE CONFIDENTIAL REPORT

THE DETERMINATION OF SPAN LOAD DISTRIBUTION AT HIGH SPEEDS BY USE OF HIGH-SPEED WIND-TUNNEL SECTION DATA

By John Boshar

SUMMARY

A tabular method is presented for determining the span load distribution at high Mach numbers by utilizing high-speed airfoil section data. The method, designated the generalized method, is an easily applied process of successive approximations by which a general application of the lifting-line theory may be used to determine the span load distribution for wings composed of sections having arbitrary lift curves. An example is given to show how this method is used. A comparison of span load distribution obtained by the generalized method using high-speed data is made with results obtained by the strip-theory method using high-speed data and by the conventional method of applying lifting-line theory, which utilizes low-speed data.

The results of the computations indicate that the loading changes associated with Mach number may be great enough to require modification in the current method of computing span loading for design purposes.

INTRODUCTION

In some recent high-speed airplane flights a number of accidents and near accidents have occurred, which could be associated, in part, with changes in wing span load distribution at high Mach numbers. These changes have been manifested by both inordinate changes in airplane stability and formation of permanent wing wrinkles at load factors lower than should be expected on the basis of static-test results.

Qualitative considerations of the effect of Mach number on two-dimensional airfoils indicate that some

changes in loading are to be expected in the usual operating lift range, because the thicker inboard sections of a typical wing would experience a compressibility stall earlier than the outboard sections and would consequently require the outboard sections to carry a greater part of the load if the lift is to be maintained. Except for some unpublished high-speed wind-tunnel results of wake measurements behind a tapered wing, which verified the conclusion that stalling occurs earlier on the root sections than on the tip sections, no direct experimental data exist on the subject and the actual magnitude of the span-loading changes has been questionable.

Although designers are aware, therefore, that changes occur in the section lift curves after the occurrence of a compressibility stall, airplane wings are still built to carry the limit loads distributed in accordance with a lifting-line theory that includes the assumption that the individual sections along the span have a constant lift-curve slope throughout the entire operating range.

The purpose of the present report is:

(1) To present a tabular method by which the lifting-line theory may be easily applied to the determination of the span load distribution of a wing, regardless of the type of section lift curves.

(2) To present, for two hypothetical wings, comparisons of the span load distribution as determined by means of

(a) The strip theory, in which high-speed wind-tunnel data are used

(b) The conventional application of the lifting-line theory, in which low-speed wind-tunnel data are used

(c) The generalized method of applying lifting-line theory, in which high-speed wind-tunnel data are used

(3) To present an example showing how the generalized method may be used to determine span load distribution at high speeds.

SYMBOLS

A	aspect ratio (b^2/S)
b	wing span
c_l	section lift coefficient
C_L	wing lift coefficient
C_{BM}	bending-moment coefficient
c	chord at any span
$\bar{c}$	mean chord
M	Mach number
m, n, r, s	constants defining limits of summations
n	load factor
q	dynamic pressure
S	wing area
V	airplane speed
w	downward component of velocity
W	airplane weight
y	distance from wing root, semispans
α	angle of attack; with subscript g, geometric; with subscript e, effective
ϵ	downwash angle
λ	constant coefficients in downwash equations

A prime used with a symbol indicates a particular value of the quantity.

METHODS OF COMPUTING SPAN LOAD DISTRIBUTION

A number of methods have been used to determine spanwise distribution of air load on airplane wings. The most primitive of these, the strip method, has been used to obtain rough solutions but, inasmuch as this method neglects the presence of downwash, it has not been considered accurate enough for design purposes. The method that is used in design accounts for the effect of downwash by an application of the lifting-line theory. This method which, for convenience, is referred to herein as the "conventional method," has been made adaptable to direct computation for the special case of lift curves that are essentially linear. For the cases in which this linearity of the lift curves is not present - , for example, near the point at which normal stall or premature compressibility stall occurs - the direct method is no longer satisfactory. For such cases, a third method of determining span load distributions, referred to herein as the "generalized method," makes use of a process of successive approximations to apply the lifting-line theory. Applications of this method are given in references 1, 2, and 3.

The discussion that follows is concerned with the strip method, the conventional method, and the generalized method of determining span load distribution with particular reference to their uses as related to the span load distribution that may be expected at high speeds.

Strip Method

In the strip theory, the assumption is that the wing is made up of airfoil strips, each of which maintains its two-dimensional (or infinite-aspect-ratio) lift characteristics. For a selected wing angle of attack the lift coefficient at each span station is determined from the section data by picking off the local lift coefficient corresponding to the geometric angle of attack at that section. Inasmuch as infinite aspect ratio is assumed, the effect of varying spanwise distribution of induced angle of attack in neutralizing any discontinuities and high gradients in the loadings is neglected. The loadings are derived by multiplying the lift coefficients at each station by the ratio of the chord at the station to the mean chord; thus, a

load coefficient $c_l\frac{c}{\bar{c}}$ is defined, which is related to the usual wing lift coefficient C_L as follows:

$$C_L = \int_0^1 c_l\frac{c}{\bar{c}}\, dy$$

The application of the strip theory requires no further explanation as it is one of the oldest methods used in predicting load distribution.

Conventional Method

The conventional method of applying lifting-line theory takes into consideration the effect of aspect ratio (the presence of downwash); it is made adaptable for computing purposes by the assumption that the individual span stations have constant lift-curve slopes. Inasmuch as airplane designers are in general familiar with both the Fourier series method and the Schrenk approximate method as given and discussed in reference 4, no details of this method are given herein.

Generalized Method

The need for more generalized methods of applying lifting-line theory (references 1, 2, and 3) arose from the fact that methods were desired that could treat cases in which either partial stall or nonlinearity in the lift curves resulted. In principle, these methods are straightforward; that is, from the fundamental downwash equation a spanwise distribution of downwash angle is found for some initial assumed loading and, from the differences between the geometric and the computed downwash angles at each station of the span, the effective angles of attack are determined. When the effective angles of attack are applied to each section lift curve, lift coefficients at each station are obtained which, when multiplied by the ratio of the chord at the station to the mean chord, define a new "check" distribution. The second assumed span loading may be taken between the first approximation and the check points (not necessarily a mean). The process is continued until the check loading coincides with that from which it was derived.

Because of the difficulty in evaluating the downwash angles, the methods of successive approximations are generally tedious. The downwash angle at a span station

is obtained by carrying through the operations indicated by the fundamental equation for the downwash angle at a spanwise point, namely

$$\epsilon' = \left(\frac{w}{V}\right)' = \frac{\sigma}{4\pi b}\int_{-1}^{1} \frac{d\left(c_l \frac{c}{\bar{c}}\right)}{dy}\,\frac{dy}{y' - y} \qquad (1)$$

The prime is used to indicate the span point at which the downwash angle is being found.

Reference 1 carries out the indicated operation by plotting the load coefficient $c_l \frac{c}{\bar{c}}$ against $1/(y' - y)$ and integrating the area to obtain the downwash. A more complicated method given in reference 2 carries out the indicated operation by plotting $\dfrac{d\left(c_l \frac{c}{\bar{c}}\right)/dy}{y' - y}$ against the span station y, and integrating to find the area. In both methods, since the denominator becomes zero when $y = y'$, the integration must exclude a small area on either side of the singularity, which is then separately considered by an approximate formula. Of these two methods, that of reference 1 is simpler because it does not depend upon the graphical determination of the slope of the loading curve. A much less laborious method was developed in reference 3, which is demonstrated in reference 5, and has been found by experience to entail only a small fraction of the labor of the methods of references 1 and 2.

The method of reference 3 is essentially as follows: The distribution of span loading is expressed by the general formula (from reference 6, equation (41))

$$c_l \frac{c}{\bar{c}} = 2A\sqrt{1 - y^2} \sum_{r=0}^{\infty} a_{2r}\, y^{2r} \qquad (2)$$

which is then substituted into the basic downwash-angle formula (equation (1)) and integrated step by step to arrive at the series

$$\epsilon = \sum_{r=0}^{\infty} a_{2r}\, g_{2r} \qquad (3)$$

where

$$g_{2r} = \sum_{s=0}^{n} \left(\frac{2n+1}{2} P_{r-s} - r P_{r-s-1} \right) y^{2s}$$

and

$$P_r = \frac{1 \times 3 \times 5 \ldots (2r-1)}{2 \times 4 \times 6 \ldots 2r}$$

At this point in the development given in reference 3 it is assumed that this downwash angle may be expressed as

$$\epsilon = \frac{1}{2A} \sum_{m=1}^{n} \lambda_m \left(c_l \frac{c}{\bar{c}} \right)_m \qquad (4)$$

and since, by equation (2), $c_l \frac{c}{\bar{c}}$ may be given in terms of $y_1, y_2, y_3 \ldots y_n$,

$$\epsilon = \sum_{m=1}^{n} y_m^{2r}\, \lambda_m \sqrt{1 - y_m^2} \sum_{r=0}^{\infty} a_{2r} \qquad (5)$$

When the assumed downwash angle given by equation (5) is compared with the downwash angle given by equation (3), the corresponding terms for the two series may be made to agree if $y_1, y_2, \ldots y_n$ and $\lambda_1, \lambda_2, \ldots \lambda_n$ satisfy the condition

$$\sum_{m=1}^{n} \lambda_m\, y_m^{2r} \sqrt{1 - y_m^{2r}} = g_{2r} \qquad (6)$$

Inasmuch as equation (5) contains only y_1, y_2, . . . y_n and λ_1, λ_2, . . . λ_n, values of y may be prescribed independently of the a_{2r} coefficients and, therefore, independently of the loading $\left(c_l \frac{c}{\bar{c}}\right)$; the problem consequently reduces to the solution of a system of simultaneous equations.

The constants for the case of five simultaneous equations (n = 5) as taken from reference 3 are given in the following table and have been determined to yield the downwash angles in degrees:

λ \ y	0	0.3	0.5	0.7	0.9
λ_1	150.10	-72.67	-16.16	21.42	-107.60
λ_2	-124.46	187.77	-73.50	-81.12	242.99
λ_3	8.83	-78.17	200.14	-10.43	-248.86
λ_4	-12.49	-10.52	-76.35	169.98	38.81
λ_5	-3.34	-5.96	-8.90	-63.64	211.65

If equation (4) is expanded to n = 5, the downwash-angle equation becomes

$$\epsilon = \frac{1}{2A}\left[\lambda_1\left(c_l\frac{c}{\bar{c}}\right)_0 + \lambda_2\left(c_l\frac{c}{\bar{c}}\right)_{0.3} + \lambda_3\left(c_l\frac{c}{\bar{c}}\right)_{0.5} + \lambda_4\left(c_l\frac{c}{\bar{c}}\right)_{0.7} + \lambda_5\left(c_l\frac{c}{\bar{c}}\right)_{0.9}\right]$$

and, for example, for $y = 0.3$

$$\epsilon = \frac{1}{2A}\left[-72.67\left(c_l\frac{c}{\bar{c}}\right)_0 + 187.77\left(c_l\frac{c}{\bar{c}}\right)_{0.3} - 78.17\left(c_l\frac{c}{\bar{c}}\right)_{0.5} - 10.52\left(c_l\frac{c}{\bar{c}}\right)_{0.7} - 5.96\left(c_l\frac{c}{\bar{c}}\right)_{0.9}\right]$$

Early experience gained in applying the methods of references 1, 2, and 3 has indicated that identical results would be obtained with each of the methods after a sufficient number of trials but the method of reference 3 was found to be much easier than the others and consequently was the method used herein. A tabular scheme was finally worked out, which enabled the span load distribution to be obtained very quickly. A sample of the computations is shown in table I.

DISCRIPTION OF WINGS AND BASIC DATA

The hypothetical wings (see fig. 1) for which the high-speed loadings were determined were both of elliptical plan form and had a thickness ratio varying from 17 percent of the chord at the root to 9 percent at the tip. One wing was assumed to be of NACA 00XX sections and the other of high-critical-speed 16-5XX sections. The notation XX is substituted for the airfoil thickness in the designation. A linear geometric twist that would most nearly introduce zero aerodynamic twist at a Mach number of 0.30 was applied to the wings. In order to accomplish this result the 16-5XX wing was given a 1° geometric washout, whereas the symmetrical 00XX wing fulfilled the condition with zero geometric twist.

The basic data for the 00XX airfoil sections were obtained from the British National Physics Laboratory and those for the 16-5XX sections from the NACA 24-inch high-speed tunnel. The pertinent facts concerning the scope of the data and the reference papers in which the material is presented are given in the following table:

BASIC DATA

Airfoil section	Angle-of-attack range (deg)	Chord (in.)	Mach number range	Approximate Reynolds number range	Reference
NACA 00XX sections					
0012-63	-4 to 12	2	0.40 to 0.725	430,000 to 780,000	7
0015-63	0 to 5.75	1.493	.30 to .80	350,000 to 500,000	8
0017-63	0 to 5.5	1.5	.30 to .80	360,000 to 500,000	9
0020-63	-2 to 14	1.2	.30 to .80	200,000 to 500,000	10
NACA 16-5XX sections					
16-506	-3.2 to 2	5	0.30 to 0.75	700,000 to 2,000,000	11
16-509	-3.8 to 3	5	.30 to .75	700,000 to 2,000,000	11
16-512	-4 to 4	5	.30 to .75	700,000 to 2,000,000	11
16-515	-2.3 to 4.5	5	.30 to .75	700,000 to 2,000,000	11
16-521	-1.6 to 4	5	.30 to .70	700,000 to 2,000,000	11

The basic section data were so plotted as to permit nonlinear interpolations of the lift curves for any of the airfoil sections along the wing. The unusual type of plot adopted was suggested by one used in reference 10 for a different purpose and was constructed as follows: For a given Mach number the usual section lift curves for various thickness ratios were plotted on the same figure. The angle-of-attack scale for each thickness was staggered a distance proportional to the airfoil thickness (heavy lines in figs. 2 to 6) and the points of equal angle of attack were then joined, producing a surface or "carpet" effect. This surface allows the lift curves to be easily interpolated for airfoil thicknesses between those represented by the basic data and, in addition, gives a pictorial representation of the airfoil family making up the wing.

The particular airfoil sections used were chosen because the data were available from the same wind tunnel for each family. The 16-5XX sections were tested through the same Reynolds number range; however, the 00XX airfoils, as shown in the tabulation of the data, were of different chords and consequently the Reynolds numbers were not the same. Also, according to reference 8, the 0015-63 airfoil section was obtained by cutting down the 0017-63 section and the end blocks were probably twisted one-fourth of 1^c relative to the new datum, giving an observed error in the results in the zero-lift angle. Nevertheless, no attempt was made to correct the basic data since it was considered that the more or less arbitrary corrections would not alter the results an amount sufficient to warrant tampering with the basic data.

As shown in the tabulation of the basic data, the Mach number range for the 0012-63 airfoil section was 0.40 to 0.725. The data for this section at $M = 0.30$ (fig. 2) are therefore shown as extrapolations. In the carpet for the case of $M = 0.75$ (fig. 6) the data for the 12-percent-thick section, however, are shown as neither basic nor extrapolated data but rather as a heavy dashed line to indicate that the line, although not from basic data, was better than the extrapolated curves because the extension of the data from 0.725 to 0.75 was slight and was made by means of an auxiliary carpet. In this carpet, which is not shown, the lift curves were plotted for the various Mach numbers of the 0012-63 airfoil and the curves were then spaced in proportion to the Mach number increments.

RESULTS OF COMPUTATIONS

Span load distribution computations using the strip-theory method and the generalized method of applying lifting-line theory were performed for each of the hypothetical wings at five or six angles of attack of the root section and for each of the five Mach numbers for which data were available, that is, from figures 2 to 6. The hypothetical wings were purposely chosen with elliptical plan form and with zero aerodynamic twist in order that the span loading which would be obtained by the conventional application of lifting-line theory (reference 4) would be elliptical at the various lift coefficients.

A sample of the computations required and the procedure followed at each value of angle of attack and Mach number to obtain the span load distribution by either the strip method or the generalized method of reference 3 is shown in table I. The computations shown apply to the 16-5XX wing for an angle of attack of 2° at the root and for a Mach number of 0.75. In this table the computations required for the strip-theory calculations are included in the first six columns of the first block. The remaining columns and blocks are required to complete the computations for the method of successive approximations. It will be noted both in the table and in figure 7, which supplements the table, that in the computations by the method of successive approximations the first approximation of the loading is assumed to be that defined by the strip theory for which the local lift coefficients are shown by the solid line in figure 6. The check points obtained for the first approximation are shown both in figure 7 and on the carpet of figure 6. Table I, in conjunction with figure 7 and figure 6, may be followed to show completely the detailed procedure.

The span load distributions obtained from each of the computations were then integrated and the results cross-plotted against wing lift coefficient C_L to obtain loadings as a function of Mach number at a number of evenly spaced wing lift coefficients equal to 0.1, 0.2, 0.3, 0.4, and 0.5. The results of the cross plots are shown in figures 8 and 9. The loadings

given in these figures were obtained both by use of the lifting-line theory and by the strip theory. The solid-line curves in these figures represent the reference (or conventional) design span loading, which has been assumed by designers not to change with Mach number.

The span loadings of figures 8 and 9 were in turn integrated to give a measure of the bending moment at the wing root and at the 50-percent span station. The results of these integrations are shown in figures 10 and 11, in which a bending-moment coefficient C_{BM} is plotted against the wing lift coefficient. The bending-moment coefficient shown in these figures is defined mathematically by the expression

$$C_{BM} = \int_{y'}^{1.0} \left(c_l \frac{c}{\bar{c}}\right) (y - y') \, dy$$

This definition requires that, at the wing root, the bending-moment coefficient equal the wing lift coefficient multiplied by the lateral center of pressure of the span load. Also, with the bending-moment coefficient defined in this manner, the magnitude of the bending moment at any station y' is given by

$$\text{Bending Moment} = \frac{C_{BM}}{4} qSb$$

DISCUSSION

With respect to the generalized method used in the span load computations it may be seen that when a systematic tabulation system is adopted, very little work would be required even in a general case. The table as given could be shortened still further because the first six columns in the second, third, and fourth approximations could be deleted. All the columns have, however, been included in this paper in order to show each step clearly. Those familiar with span load computations will easily recognize that the amount of work is less than that required by the Fourier series method of reference 4 and is only slightly more than that required by the optional but shorter Schrenk approximate method that is included therein.

It will be noted that, although far more complete basic section data were available for the families chosen than for other airfoil families, the data are still rather limited in scope both as to the Mach number and the lift-coefficient range obtained. For this reason it is impossible to illustrate either the effects of Mach number on span load changes near values of $M = 0.85$ that some modern airplanes have reached or to illustrate changes that occur with even moderately high lift coefficients. Examination of the results given in any one of figures 8 through 11 indicates that changes in loading occur rapidly for the 16-5XX wing at a Mach number above 0.7 and for the 00XX wing at a Mach number above 0.6 and a lift coefficient above 0.4. The highest value of Mach number for which data are available is only 0.75. In the case of the 00XX wing, sufficient section data are available at this Mach number to allow computations to be made to a wing lift coefficient of only 0.2 and for the 16-5XX wing to a wing lift coefficient of 0.5.

From qualitative considerations it would be expected that the span load center for a wing composed of a consistent family of sections might shift either inboard or outboard, depending upon the combination of Mach number and angle of attack at which the wing is operating. At high Mach numbers and low to moderate lift coefficients, as shown by the results of the present analysis, the early stall of the thicker inboard sections of the wing produces an outboard shift of the center of load. At relatively low Mach numbers and high angles of attack, however, the loading may shift inboard because of the earlier stall of the thinner sharp-nosed outboard sections. The span load center could also move inboard when the wing operates at low angles of attack and near critical Mach numbers, because the higher negative pressures over the thicker inboard sections would then be expanded more than the lower pressures of the thinner tip sections. The basic data are not of sufficient range to show the inboard shift of the center of load caused by tip stalling; however, the inboard shift as caused by reduction of pressure over the upper surface of the root sections is indicated by the results given in figure 8, in which the loading may be noted to move inboard for the 16-5XX wing at lift coefficients below 0.20 at $M = 0.70$.

For a given rigid wing the shift in span loading that occurs at high Mach numbers depends on the change with Mach number of the relative positions of the lift curves for the sections making up the wing. The relative positions of the section lift curves at various Mach numbers may be clearly noted from the carpet plots (figs. 2 to 6); these plots are particularly advantageous for presenting a quick impression of the high-speed performance of the wing. For instance, for the 00XX wing at a Mach number of 0.70 (fig. 5) the relative positions of the section lift curves for the 9-percent and 17-percent-thick sections at low angles of attack are almost the same as for the wing at a Mach number of 0.30 (fig. 2) and little change in loading is therefore to be expected at these angles. The relative positions of the section lift curves for the inboard and outboard sections change, however, as the angles of attack increase, and the span loading changes should become more severe with increasing angle of attack. This conclusion is borne out in the bending-moment-coefficient curves of figure 11, which show that the bending-moment coefficient for $M = 0.70$ increases with lift coefficient. For the 16-5XX wing at a Mach number of 0.75 (fig. 6), all the section lift curves of the thicker sections have been displaced downward, indicating that the inboard sections carry less lift but, inasmuch as the slope changes little between the outboard and inboard sections throughout the angle-of-attack range, the increase in bending-moment coefficient should be constant with angle of attack. Figure 10 verifies this deduction.

From the foregoing discussion it is evident that the manner in which changes in the span loading occur is dependent upon the airfoil sections and other geometric characteristics of the wing. For the two wings considered, the changes of span loading with Mach number brought about in the first case a constant bending-moment-coefficient increase over the low-speed value with increasing lift coefficient and in the second case a gradual increase over the low-speed value with increasing lift coefficient. From an examination of the carpets of different wings at both low and high Mach numbers, the family of airfoils may be selected that has the most favorable span-load-change characteristics.

When related to possible flight conditions, the bending-moment increases indicated in figures 10 and 11 are sufficiently high that the safe load factor would be considerably diminished. Figures 12 and 13 have been

prepared to illustrate this point. Figure 12 shows the variation of bending-moment coefficient with load factor at two spanwise stations for a pursuit airplane equipped with a 16-5XX wing having a loading of 40 pounds per square foot and a Mach number of 0.75 at 10,000 feet. Figure 13 shows the same results for the airplane equipped with the 00XX wing at a Mach number of 0.70 at 10,000 feet. Under ordinary conditions the wings would be designed to sustain the bending moments corresponding to a load factor of 8g and bending-moment coefficients of 0.045 and 0.235 at the 50 percent and root stations, respectively. Both the strip theory and the generalized lifting-line theory show that these values of bending-moment coefficient would be obtained at values of the load factor substantially less than 8g.

In the strip theory, no consideration is given the effect of induced flow in leveling the load gradients along the span; the loads obtained with this method are therefore more severe than those obtained when the generalized lifting-line theory is used. For the two hypothetical wings, however, even this simple strip theory gives results closer to the high-speed loading and is more conservative than is the conventional method used in design.

It should be noted that the downwash equation has been assumed to apply for compressible as well as for incompressible flow. To a first approximation this assumption is reasonable because, regardless of the type of flow in which a given lift is realized, the principle of induction would still apply. Even substantial changes in the downwash angle due to compressibility should, however, not be expected to greatly alter the span loadings, as these changes would occur all along the span and, for a given family of section lift curves, it is the change of the form of the downwash-angle distribution along the span which influences the span load distribution most.

The results given herein were obtained for a rigid, smooth wing, without fuselage and nacelles. In an actual case the critical condition may occur at lower Mach numbers because of flow disturbances caused by protuberances near the root station, such as inspection plates and wing fold doors, and by fuselages and nacelles.

The effect of wing nacelle and fuselage interference on the span loading may be taken into account, to a first order at least, by considering that these items cause a change in the Mach numbers of the sections along the wing span. This effect diminishes as the distance is increased from the interfering body. Reference 12 indicates a method by which the increments in Mach number caused by interfering bodies such as nacelles and fuselages may be determined. The application of computed increments in a practical case, however, suggests that the basic data given in the carpets of figures 2 to 6 be plotted to obtain five charts, one for each thickness at the selected spanwise stations, with the scales offset to give the Mach number instead of the thickness as the parameter on each chart. The lack and uncertainty of section data at high speeds on various families, however, make the carrying out of such a detailed procedure hardly worthwhile at the present time.

CONCLUDING REMARKS

The spanwise distribution of load on an airplane wing at high speeds may be determined by means of a generalized method of applying lifting-line theory. The results of applying such a method show that the bending-moment changes that can occur at high Mach numbers may be sufficiently great to render necessary a modification in the procedure now used in computing span loading.

In order to determine the validity of the general application of the lifting-line theory, it is recommended that measurements of the span load distribution be made in a high-speed wind tunnel on a wing composed of airfoil sections for which the two-dimensional high-speed characteristics are available at fairly high Mach numbers and at high angles of attack.

Langley Memorial Aeronautical Laboratory,
National Advisory Committee for Aeronautics,
Langley Field, Va.

REFERENCES

1. Fage, A.: On the Theory of Tapered Aerofoils. R. & M. No. 806, British A.R.C., 1923.

2. Jacobs, Eastman N., and Sherman, Albert: Wing Characteristics as Affected by Protuberances of Short Span. NACA Rep. No. 449, 1933.

3. Tani, Itiro: A Simple Method of Calculating the Induced Velocity of a Monoplane Wing. Rep. No. 111 (vol. IX, 3), Aero. Res. Inst., Tokyo Imperial Univ., Aug. 1934.

4. Anon: Spanwise Air-Load Distribution. ANC-1(1), Army-Navy-Commerce Committee on Aircraft Requirements. U.S. Govt. Printing Office, April 1938.

5. Wieselsberger, C.: On the Distribution of Lift across the Span near and beyond the Stall. Jour. Aero. Sci., vol. 4, no. 9, July 1937, pp. 363-365.

6. Prandtl, L.: Applications of Modern Hydrodynamics to Aeronautics. NACA Rep. No. 116, 1921.

7. Hilton, W. F., Cowdrey, C. F., and Hyde, G. A. M.: Tests of NACA 0012-63 Aerofoil in the High Speed Tunnel. 4715, Ae. 1710 N.P.L., Sept. 24, 1940.

8. Hilton, W. F., Cowdrey, C. F., and Hyde, G. A. M.: Tests of N.A.C.A. 0015-63 Section in the High Speed Tunnel. 4738, Ae. 1717, N.P.L., Oct. 9, 1940.

9. Hilton, W. F., Cowdrey, C. F., and Hyde, G. A. M.: Tests of NACA 0017-63 Aerofoil in the High Speed Tunnel. 4804, Ae. 1739, N.P.L., Nov. 11, 1940.

10. Hilton, W. F.; An Experimental Analysis of the Lift of 18 Aerofoils at High Speeds. 6062, F. M. 544, Ae. 2061, N.P.L., Aug. 31, 1942.

11. Stack, John: Tests of Airfoils Designed to Delay the Compressibility Burble. NACA TN No. 976, Dec. 1944 (Reprint of ACR, June 1939.)

12. Robinson, Russell G., and Wright, Ray H.: Estimation of Critical Speeds of Airfoils and Streamline Bodies. NACA ACR, March 1940.

TABLE I

COMPUTATIONS REQUIRED IN DETERMINATION OF SPAN LOADING

BY METHOD OF REFERENCE 3 FOR 16-5XX WING

[Angle of attack at root = 2°, M = 0.75]

First approximation

1	2	3	4	5	6	7	8	9	10	11	12	Check 13	14	15	16	17
y	Airfoil thickness (percent chord)	α_g (deg)	c_l	$\frac{c}{\bar{c}}$	$c_l\frac{c}{\bar{c}}$	$\frac{(6)}{2A}$	λ_m × column 7					ϵ (deg)	α_e (deg)	c_l	$c_l\frac{c}{\bar{c}}$	$c_l\frac{c}{\bar{c}}$
							0	0.3	0.5	0.7	0.9					
0	17.0	2.0	0.161	1.273	0.205	0.0171	2.57	-1.24	-0.28	0.37	-1.84	-1.60	3.60	0.320	0.407	0.260
0.3	14.6	1.7	.309	1.215	.375	.0313	-3.90	5.88	-2.30	-2.54	7.61	1.08	.62	.210	.255	.331
.5	13	1.5	.412	1.103	.454	.0379	.33	-2.96	7.59	-.40	-9.43	1.68	-.18	.267	.295	.368
.7	11.4	1.3	.530	.909	.482	.0402	-.50	-.42	-3.07	6.83	1.56	2.38	-1.08	.315	.286	.355
.9	9.8	1.1	.636	.555	.353	.0295	-.10	-.18	-.26	-1.88	6.24	4.13	-3.03	.126	.067	.209
							-1.60	1.08	1.68	2.38	4.13					

Second approximation

												Check				
0	17.0	2.0		1.273	0.260	0.0217	3.26	-1.58	-0.35	0.46	-2.33	-0.34	2.34	0.200	0.255	0.255
0.3	14.6	1.7		1.215	.331	.0276	-3.44	5.18	-2.03	-2.24	6.71	.79	.91	.235	.286	.315
.5	13	1.5		1.103	.368	.0307	.27	-2.40	6.14	-.32	-7.64	1.34	.16	.291	.321	.350
.7	11.4	1.3		.909	.355	.0296	-.37	-.31	-2.26	5.03	1.15	1.82	-.52	.371	.337	.341
.9	9.8	1.1		.555	.209	.0175	-.06	-.10	-.16	-1.11	3.70	1.59	-.49	.480	.266	.231
							-.34	.79	1.34	1.82	1.59					

Third approximation

												Check				
0	17.0	2.0		1.273	0.255	0.0213	3.20	-1.55	-0.34	0.46	-2.29	-0.23	2.23	0.188	0.239	0.246
0.3	14.6	1.7		1.215	.315	.0263	-3.27	4.94	-1.93	-2.13	6.39	.69	1.01	.244	.296	.305
.5	13	1.5		1.103	.350	.0292	.26	-2.28	5.84	-.30	-7.27	1.22	.28	.303	.334	.341
.7	11.4	1.3		.909	.341	.0285	-.36	-.30	-2.18	4.86	1.11	1.64	-.34	.385	.350	.342
.9	9.8	1.1		.555	.231	.0193	-.06	-.12	-.17	-1.23	4.08	2.02	-.92	.419	.233	.232
							-.23	.69	1.22	1.64	2.02					

Fourth approximation

												Check				
0	17.0	2.0		1.273	0.246	.0205	3.08	-1.49	-0.33	0.44	-2.21	-0.26	2.26	0.191	0.243	
0.3	14.6	1.7		1.215	.305	.0255	-3.17	4.79	-1.87	-2.07	6.20	.65	1.05	.250	.304	
.5	13	1.5		1.103	.341	.0282	.25	-2.23	5.70	-.30	-7.09	1.15	.35	.310	.342	
.7	11.4	1.3		.909	.342	.0286	-.36	-.30	-2.18	4.86	1.11	1.70	-.40	.377	.343	
.9	9.8	1.1		.555	.232	.0194	-.06	-.12	-.17	-1.23	4.11	2.12	-1.02	.405	.225	
							-.26	.65	1.15	1.70	2.12					

Column

3 Geometric angle of attack.
4 First assumption; lift coefficients corresponding to α_g (strip theory) from figure 6.
6 Assumed span loading coefficient.
8 to 12 Column 7 × Tani's constants λ for y = 0, 0.3, 0.5, 0.7, and 0.9.
13 Summation of column 8, 9, 10, 11, and 12.
14 Effective angle of attack (column 3 - column 13).
15 Lift coefficient corresponding to column 14 taken from carpet (as shown in figure 6).
16 "Check" load coefficient, column (15) × column (5).
17 Load coefficients from curve faired between values from columns (6) and (16) (as shown in figure 7) and entered in next approximation under column 6.

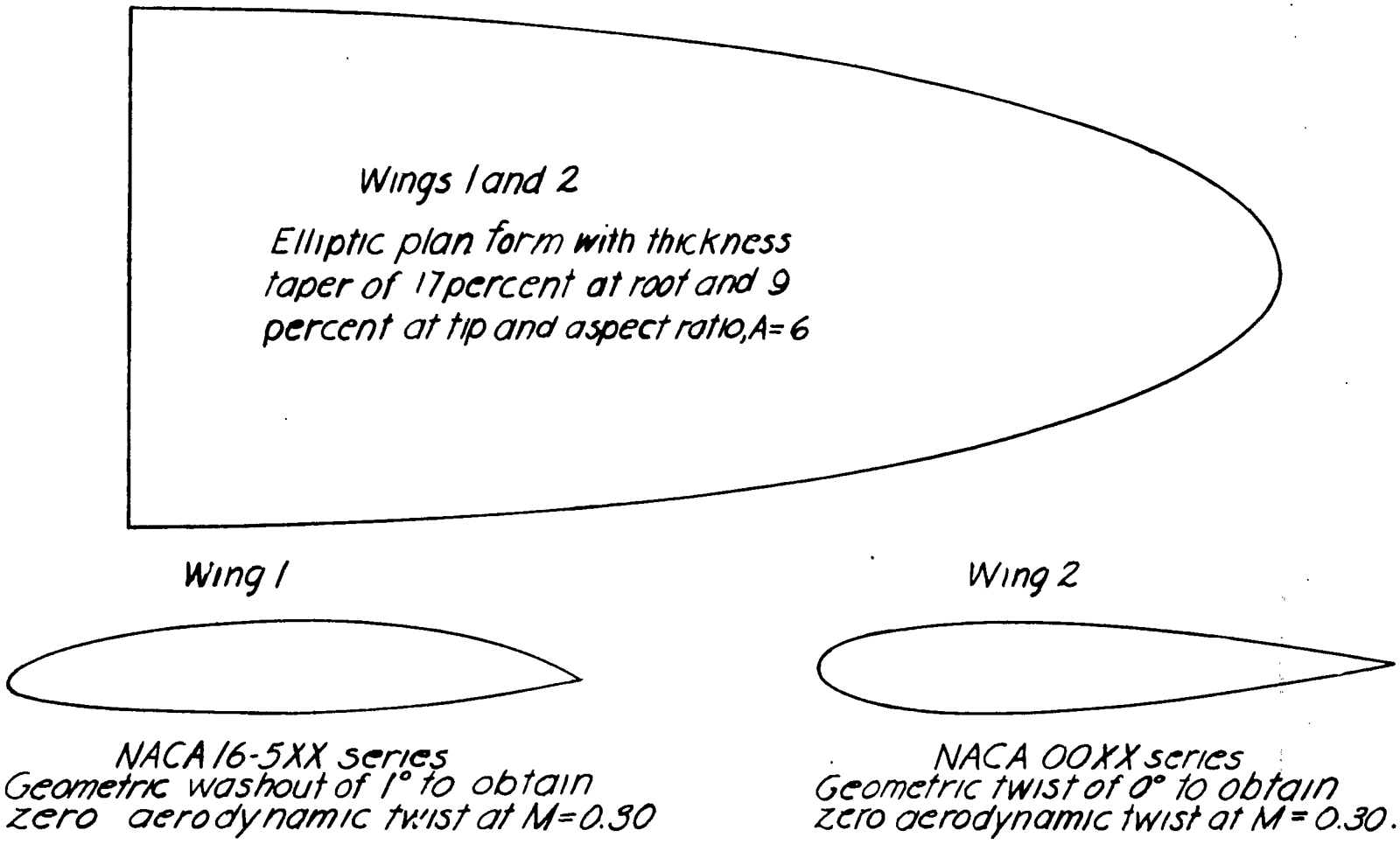

Figure 1.- Wings of different basic sections used for analysis of span load distributions at high speeds.

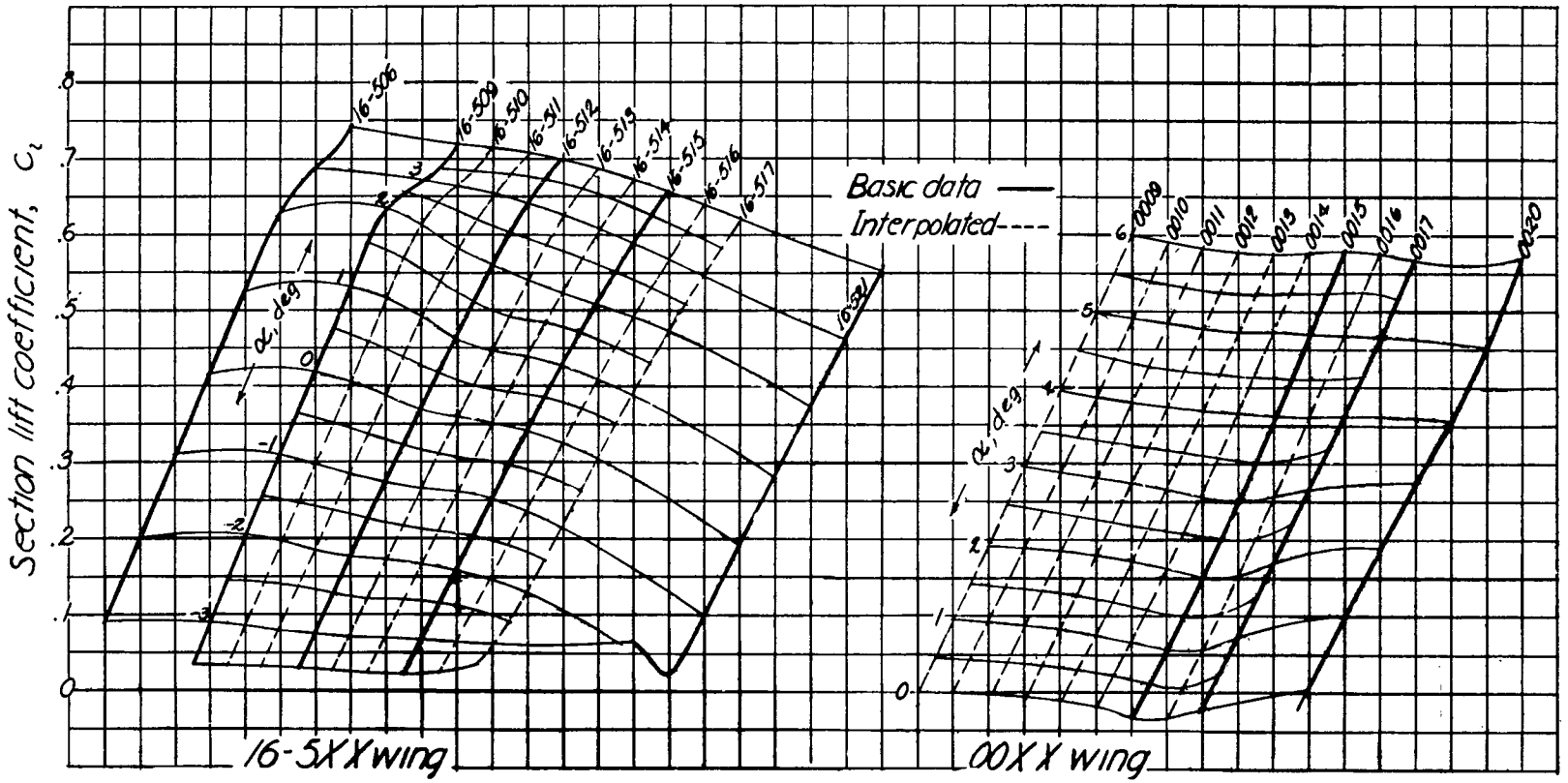

Figure 2. - Carpets for interpolation of basic section data of 16-5XX and 00XX airfoils. M=0.30.

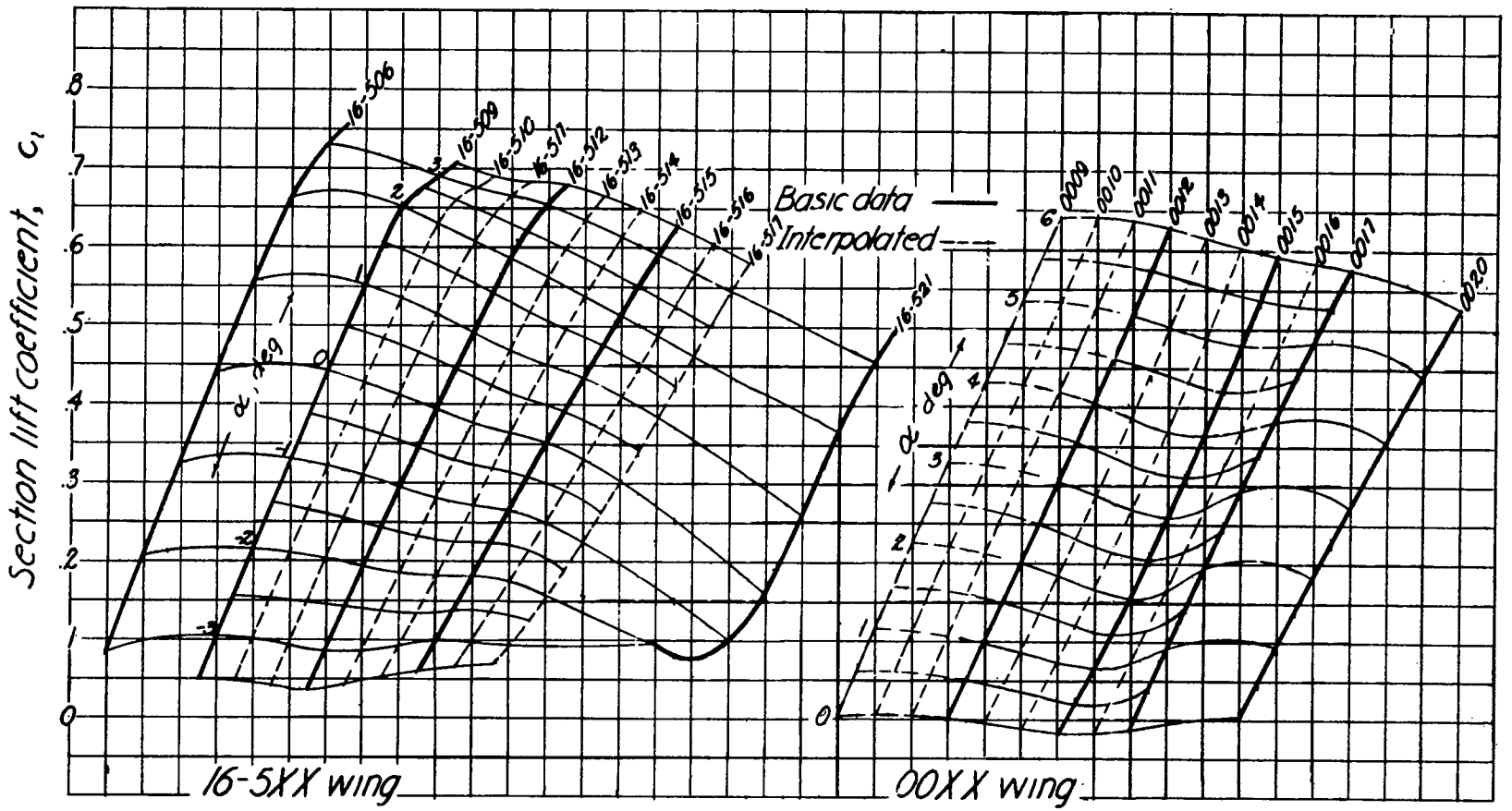

Figure 3.- Carpets for interpolation of basic section data of 16-5XX and 00XX airfoils. M = 0.45.

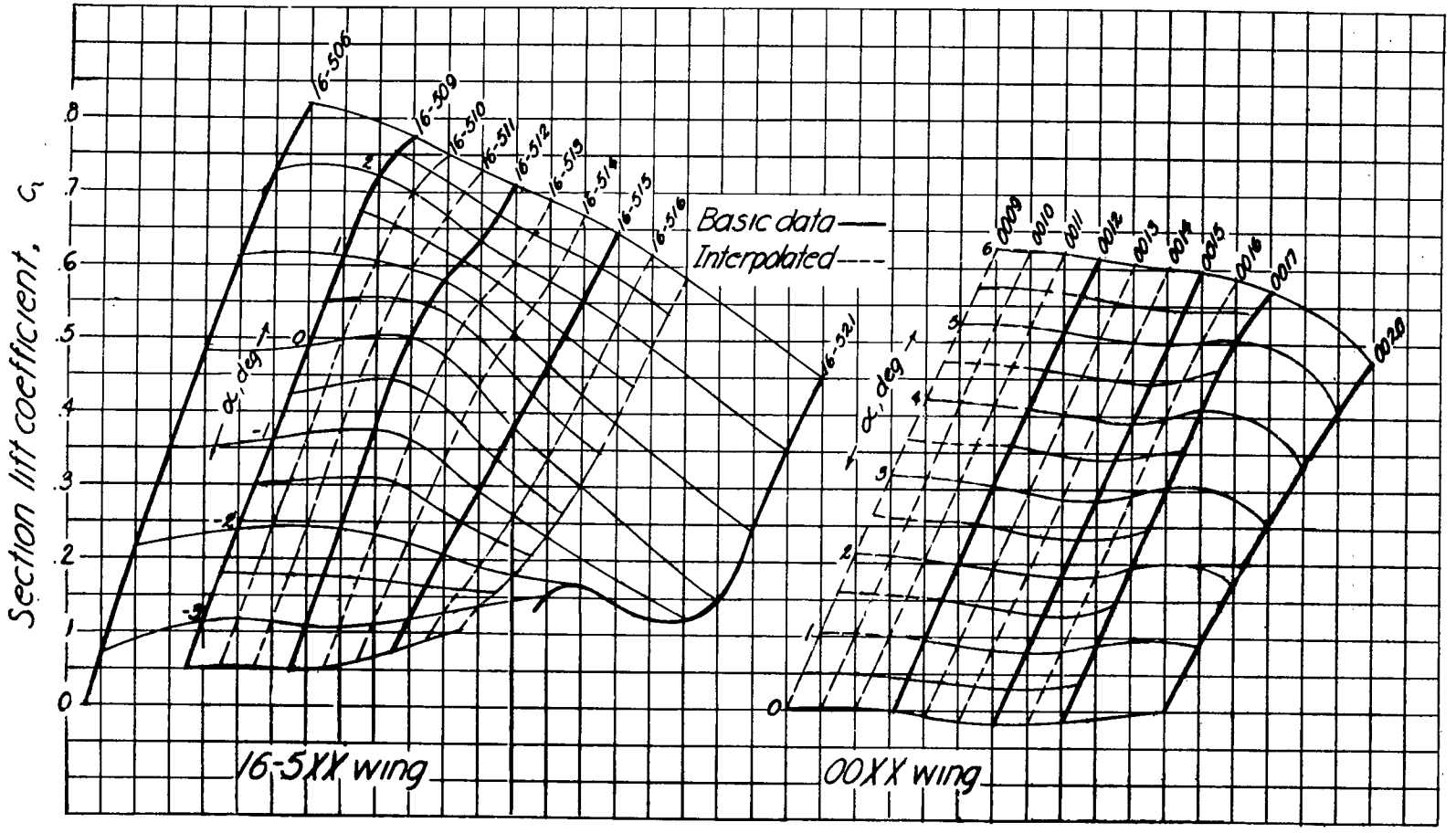

Figure 4.- Carpets for interpolation of basic section data of 16-5XX and 00XX airfoils. M=0.60

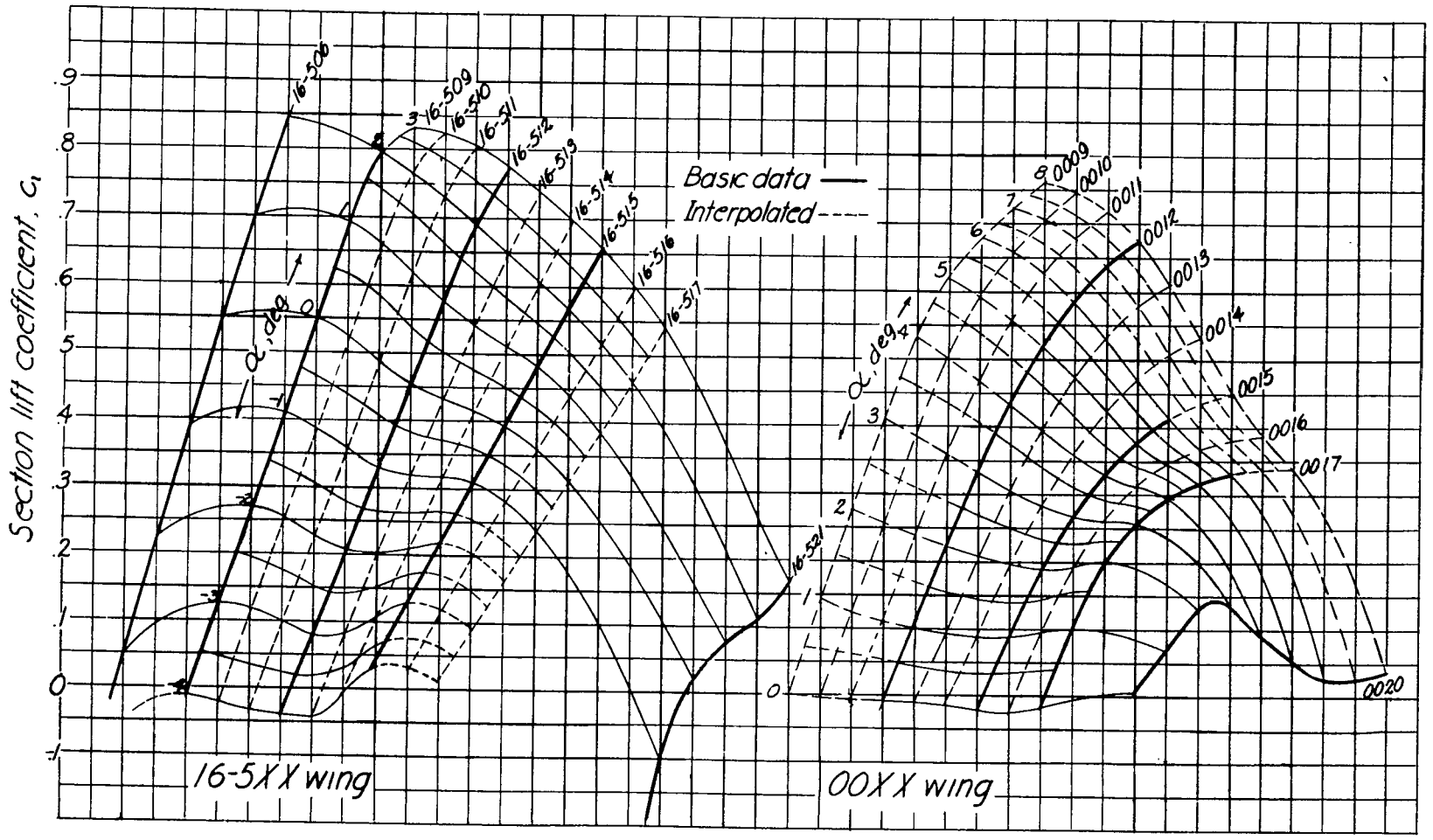

Figure 5.- Carpets for interpolation of basic section data of 16-5XX and 00XX airfoils. M=0.70

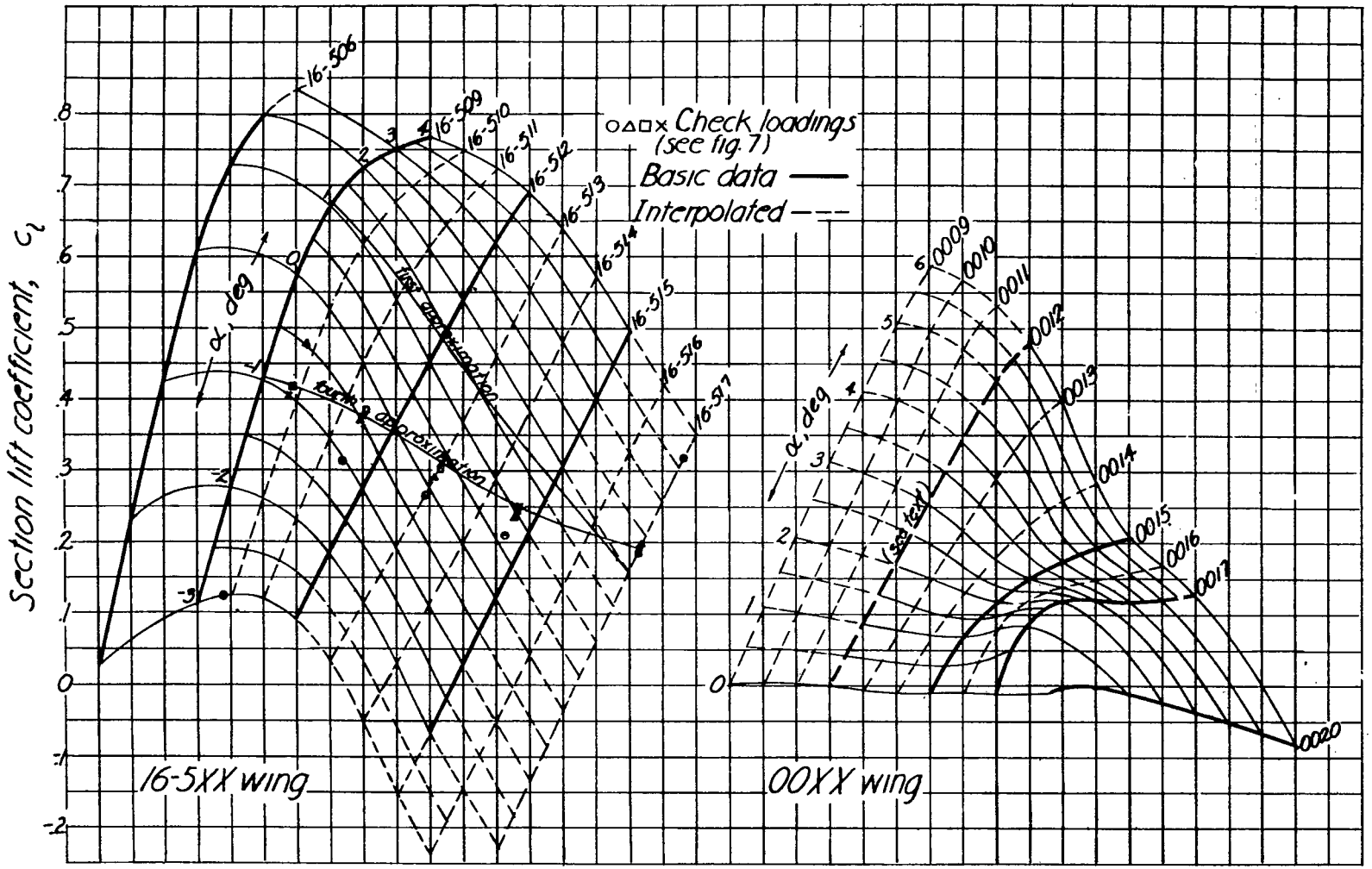

Figure 6.- Carpets for interpolation of basic section data of 16-5XX and 00XX airfoils. $M = 0.75$.

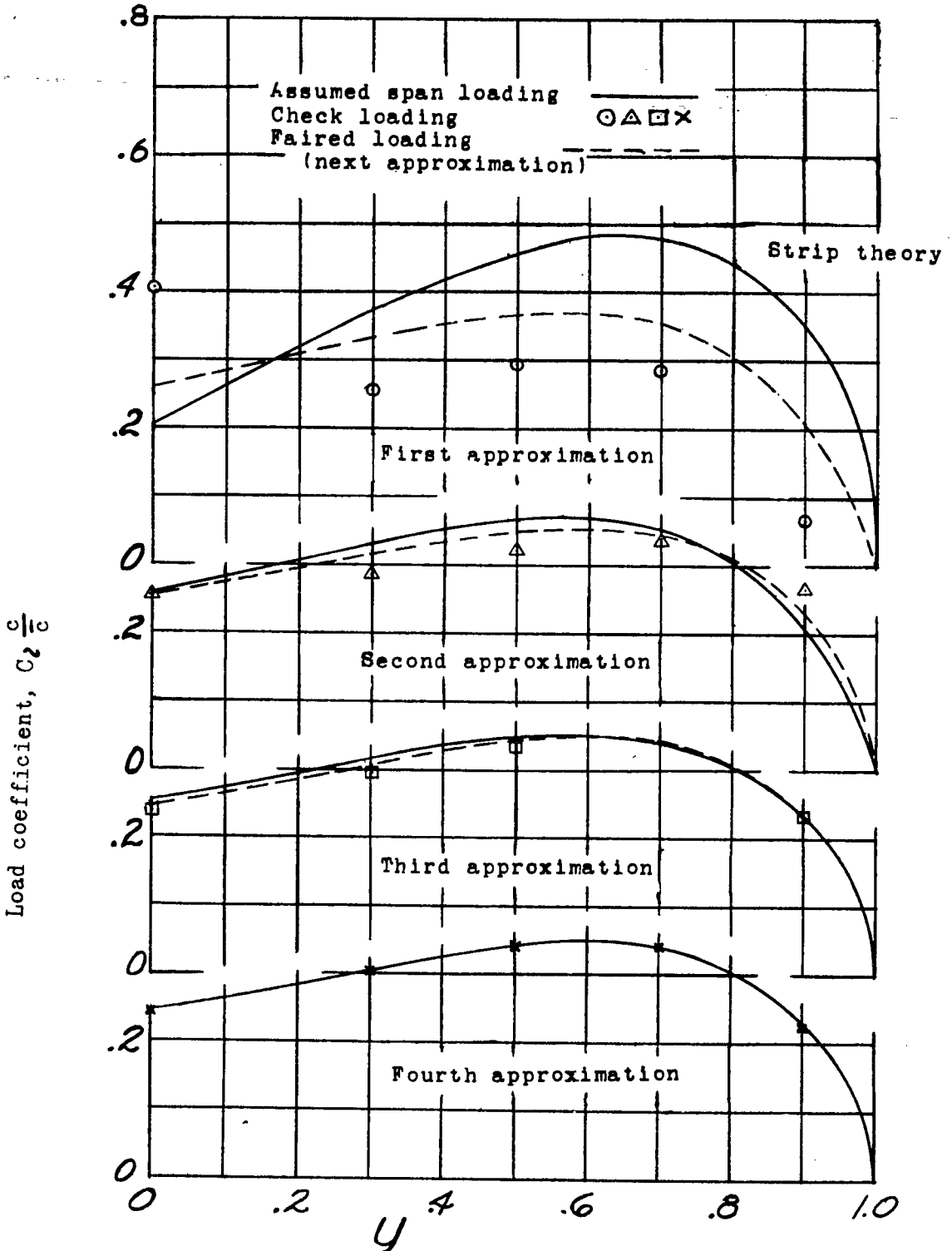

Figure 7.-Sample determination of span loading on 16-5XX wing by successive approximations. (see table I)

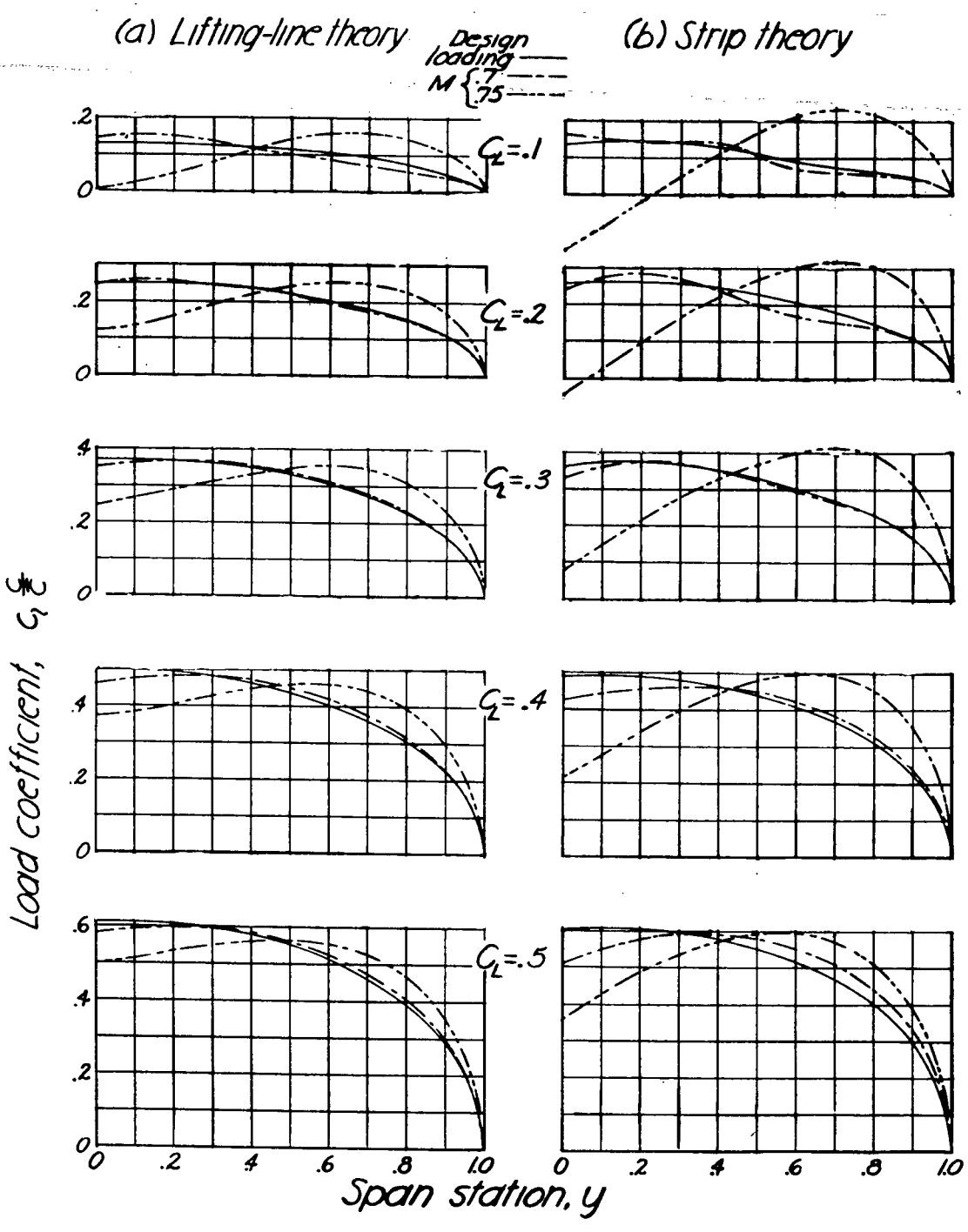

Figure 8.- The effect of Mach number on span loading for various lift coefficients on an NACA 16-5XX wing.

L-4336

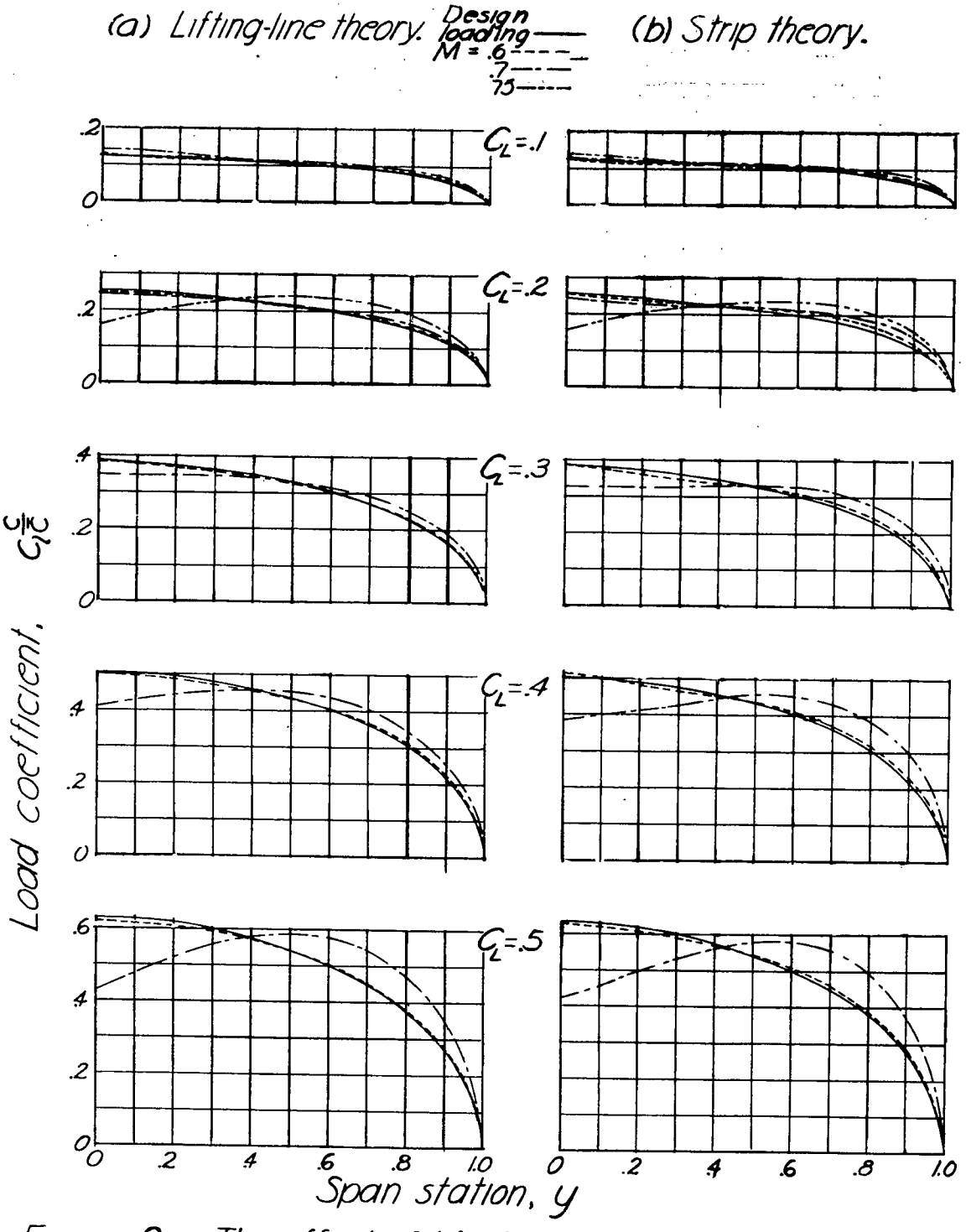

Figure 9 .- The effect of Mach number on span loading for various lift coefficients on an NACA 00XX wing.

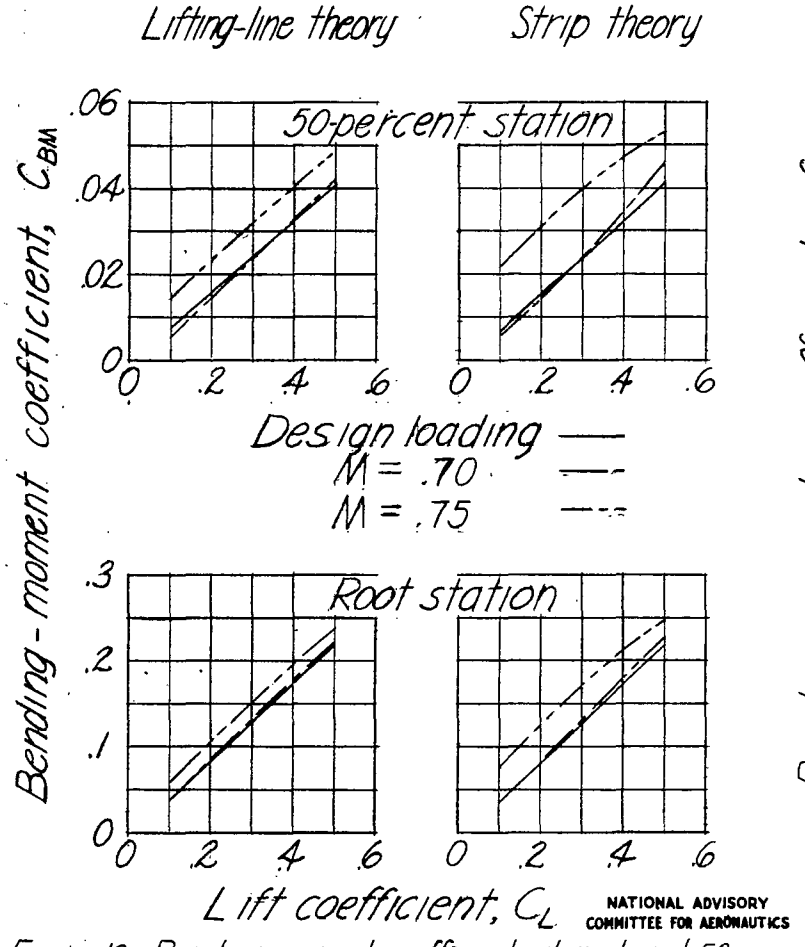

Figure 10.- Bending-moment coefficient at root and 50-percent span stations against lift coefficient. 16-5XX wing.

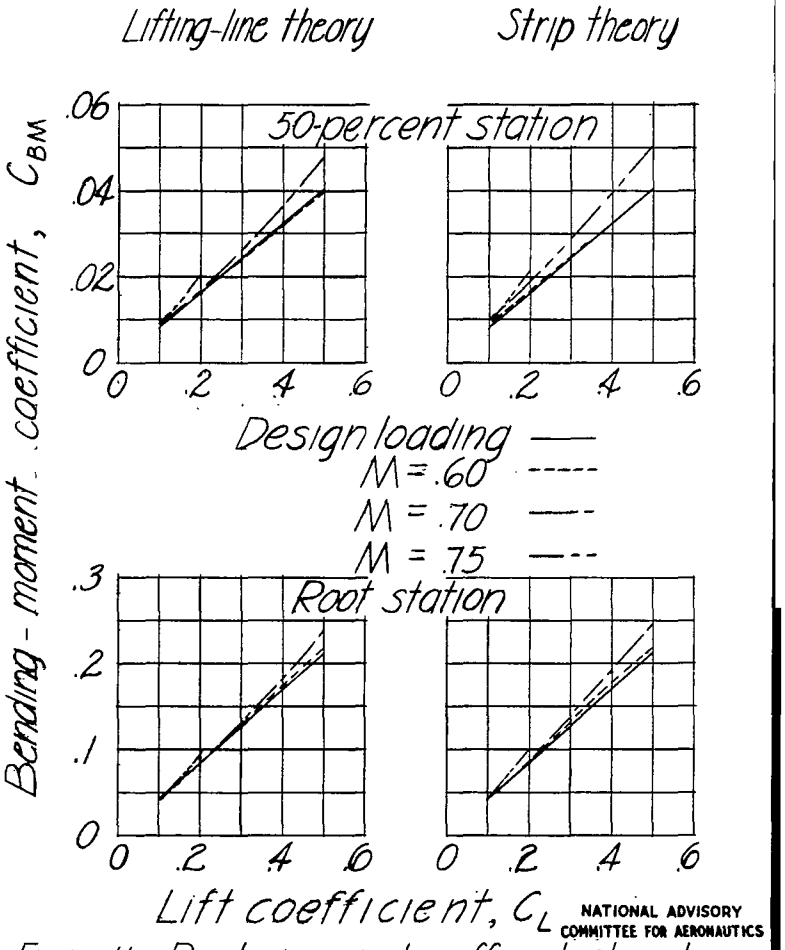

Figure 11.- Bending-moment coefficient at root and 50-percent span stations against lift coefficient. 00XX wing.

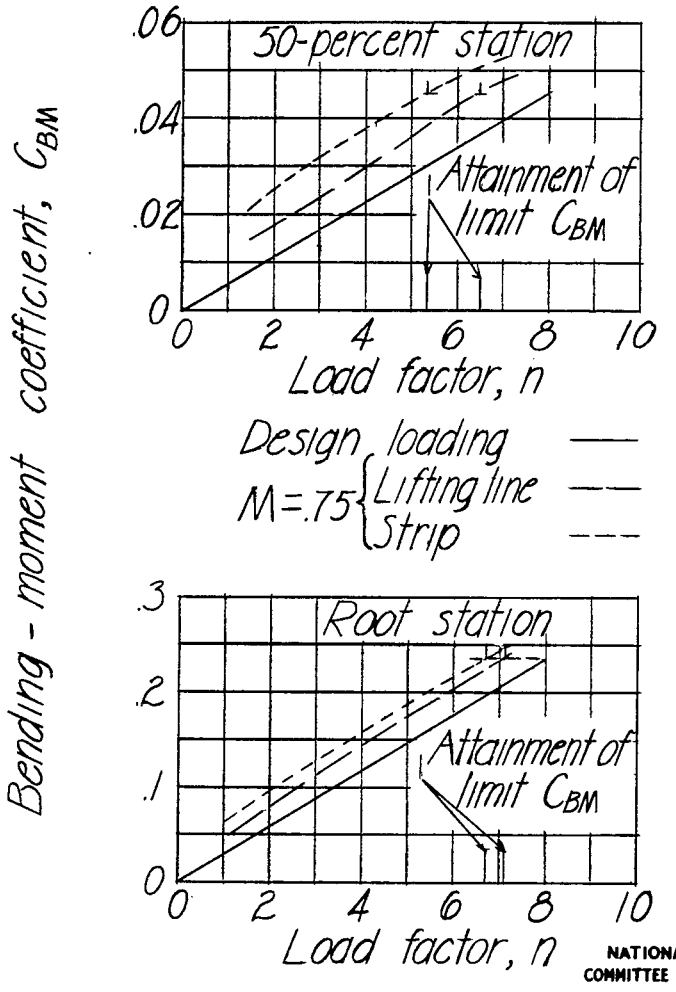

Figure 12.—Bending-moment coefficient at root and 50-percent span station against load factor at 10,000 feet for W/S=40. 16-5XX wing.

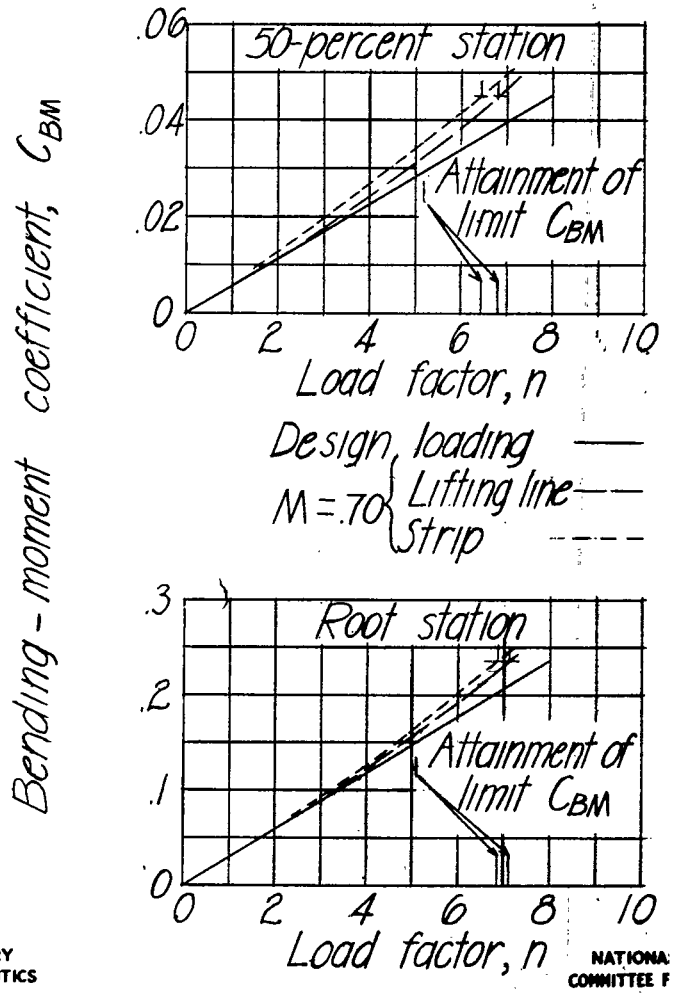

Figure 13.—Bending-moment coefficient at root and 50-percent span station against load factor at 10,000 feet for W/S=40. 00XX wing.